applied sciences

MDPI

Article

Influence of Rutin, Sinapic Acid, and Naringenin on Binding of Tyrosine Kinase Inhibitor Erlotinib to Bovine Serum Albumin Using Analytical Techniques Along with Computational Approach

Tanveer A. Wani [1,*], Ahmed H. Bakheit [1], Seema Zargar [2], Arwa Ishaq A. Khayyat [2] and Abdulrahman A. Al-Majed [1]

[1] Department of Pharmaceutical Chemistry, College of Pharmacy, King Saud University, P.O. Box 2457, Riyadh 11451, Saudi Arabia; abujazz76@gmail.com (A.H.B.); almajed99@yahoo.com (A.A.A.-M.)
[2] Department of Biochemistry, College of Science, King Saud University, P.O. Box 22452, Riyadh 11451, Saudi Arabia; szargar@ksu.edu.sa (S.Z.); aalkhyyat@ksu.edu.sa (A.I.A.K.)
* Correspondence: twani@ksu.edu.sa

Abstract: Flavonoid-containing food supplements are widely used as antioxidants, and the continuous use of these supplements with other drugs can lead to clinically significant interactions between these and other drugs. The medications in systemic circulation are mainly transported by serum albumin, a major transport protein. This study evaluated the interactions of rutin (RUT), naringenin (NAR), and sinapic acid (SIN) with the most abundant transport protein, bovine serum albumin (BSA), and the anticancer drug, the tyrosine kinase inhibitor Erlotinib (ETB), using various analytical methods. Interaction between multiple types of ligands with the transport proteins and competition between themselves can lead to the bound ETB's displacement from the BSA-binding site, leading to elevated ETB concentrations in the systemic circulation. These elevated drug fractions can lead to adverse events and lower tolerance, and increased resistance to the therapeutic regimen of ETB. The experimental and computational methods, including molecular-docking studies, were used to understand the molecular interactions. The results suggested that the complexes formed were utterly different in the binary and the ternary system. Furthermore, comparing the ternary systems amongst themselves, the spectra differed from each other. They thus inferred that complexes formed between BSA-ETB in the presence of each RUT, NAR, and SIN separately were also different, with the highest value of the reduction in the binding energy in RUT, followed by SIN and then NAR. Thus, we conclude that a competitive binding between the ETB and these flavonoids might influence the ETB pharmacokinetics in cancer patients by increasing ETB tolerance or resistance.

Keywords: Erlotinib; bovine serum albumin; fluorescence quenching; binding interaction; rutin; naringenin; sinapic acid

Citation: Wani, T.A.; Bakheit, A.H.; Zargar, S.; Khayyat, A.I.A.; Al-Majed, A.A. Influence of Rutin, Sinapic Acid, and Naringenin on Binding of Tyrosine Kinase Inhibitor Erlotinib to Bovine Serum Albumin Using Analytical Techniques Along with Computational Approach. *Appl. Sci.* **2022**, *12*, 3575. https://doi.org/10.3390/app12073575

Academic Editor: Antony C. Calokerinos

Received: 17 March 2022
Accepted: 30 March 2022
Published: 31 March 2022

1. Introduction

Serum albumin protein is the abundant constituent of the plasma and plays a pivotal role in transporting endogenous and/or exogenous ligands [1]. Ligands bind to the albumin, which influences both the pharmacodynamics and pharmacokinetics of the ligand [2,3]. All the drugs reversibly bind to the plasma proteins, and their effect generally is dependent on the free drug fraction present in the systemic circulation. The binding capacity of the drug to plasma proteins is a major consideration for selecting the dosage of the drug. Thus, the free drug fraction present in the plasma is generally responsible for the drug's therapeutic effect [4–6].

The BSA is structurally homologous and presents a 75.6% sequence similarity to human serum albumin (HSA). Therefore, BSA was chosen in the present study as a substituent to HSA since it has the same ligand-binding properties and is readily available and

cost-effective [7,8]. BSA has three primary ligand-binding sites in subdomain IIA, IIIA, and IB [9–12]. The intrinsic fluorescence of BSA, which is associated with two tryptophan amino acids (Trp-134 and Trp-213), is generally used for studies on drug–protein interactions.

Drugs reversibly bind to the plasma proteins, and the free drug fraction present in the systemic circulation at a given time is considered responsible for its therapeutic effect. Therefore, a competition between two or more drugs can occur upon their coadministration for the same BSA-binding site. This phenomenon leads to the competition or displacement of bound drugs to their binding sites, resulting in altered pharmacokinetics [13,14]. In addition, ligands binding to BSA might also cause conformational changes in the protein molecule, thus altering their ligand-binding phenomenon [15,16].

Coadministration of drugs might lead to elevated plasma concentrations of the displaced drug because of competition or displacement from the binding site. Thus, interaction at the serum albumin-binding level might cause toxic effects in the case of narrow therapeutic index drugs. These interactions may also lead to a higher incidence of adverse events, higher volume of distribution, or a subtherapeutic response due to shorter elimination half-life [17].

Phenolic-compound flavonoids are commonly used as antioxidants in nutritional supplements [18]. A citrus flavonoid glycoside, RUT, is a potent antioxidant with anti-inflammatory activities [18,19]. RTN is believed to have an anticancer potential and is recommended as a dietary supplement to prevent and manage cancer [20]. Another citrus flavonoid glycoside, NAR, which has high antioxidant potential, is also used as a dietary supplement [21] and has anticancer properties [22]. The hydroxycinnamic-acid derivative sinapic acid (SIN) has shown anticancer activity by various mechanisms, including enzyme biotransformation (Figure 1) [23].

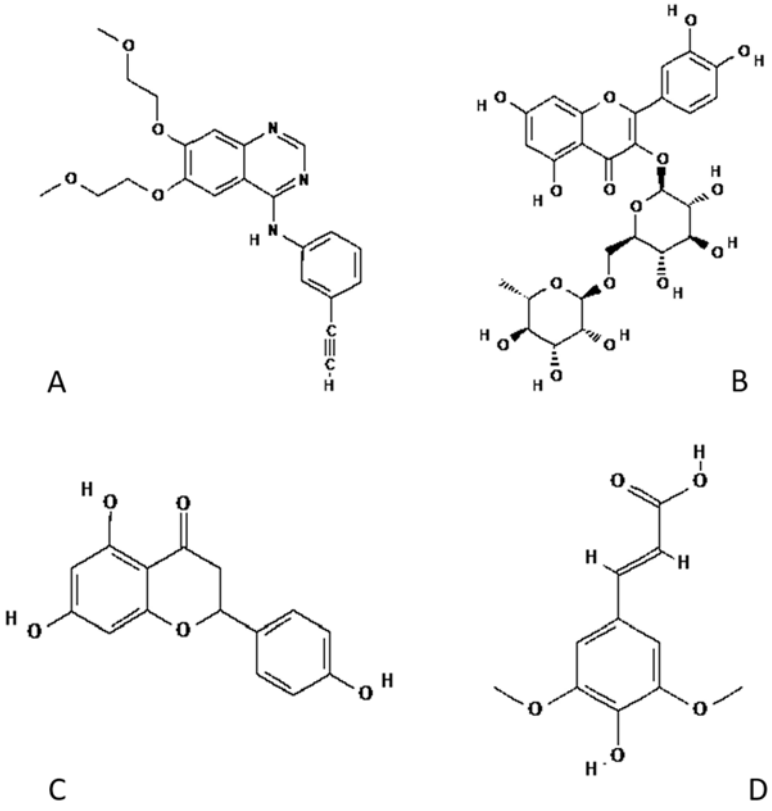

Figure 1. The chemical structures of (**A**): ETB; (**B**): RUT; (**C**): NAR; (**D**): SIN.

The ETB (Figure 1) is an ATP-competitive quinazoline derivative that works by binding to the epidermal growth factor receptor (EGFR), disabling its phosphorylation ability leading to apoptosis [24]. It is a tyrosine kinase inhibitor used to treat non-small-cell lung

cancer (NSCLC). In 2013, ETB was approved by FDA for use as a first-line treatment of NSCLC in patients whose tumors harbor EGFR exon-19 in-frame deletions or exon-21 (L858R) mutations. (20-b) [25]. Coadministering RTN, NAR, and SIN either as dietary supplements or as their presence in fruits or vegetables and ETB to treat NSCLC might cause some interactions, resulting in altered therapeutic benefit or higher incidence of adverse events to ETB [24,26].

ETB's pharmacokinetics might be influenced by simultaneous administration of ETB along with these flavonoids [26,27]. The present study investigates the effect of RUT, NAR, and SIN on the binding of ETB and BSA as a model protein. Since the drugs might compete for the same binding site, the studied flavonoids might displace ETB from its BSA-binding site, causing a higher free ETB concentration. The ETB side effects hinder the adherence to the therapeutic regimen, and these in turn are related to the plasma concentration of ETB. Thus, our study explored the in vitro influence of RUT, NAR, and SIN on ETB binding to serum albumin.

2. Materials and Methods

2.1. Chemicals

ETB was procured from Weihua Pharma Co., Limited (Hangzhou, Zhejiang, China) and the fatty-acid-free BSA from Sigma-Aldrich (St. Louis, MO, USA). RUT, NAR, and SIN were obtained through the National Scientific company (Riyadh, Saudi Arabia). The stock solutions for the standard drugs were prepared in dimethyl sulfoxide and then diluted with (phosphate buffer saline) PBS. The water used to prepare phosphate buffer was Type I water obtained from the Millipore system (Burlington, MA, USA).

2.2. Fluorescence Measurements

The fluorescence spectral measurements were carried out with an FP-8200 spectrofluorometer (JASCO, Hachioji, Tokyo, Japan). The instrument was set at the slit width of 5 nm quartz cell holder. The required spectra after the correction of the inner filter effects were evaluated by the equation [28]:

$$F_{cor} = F_{obs} \times e^{(A_{ex}+A_{em})/2}$$

where F_{obs}, F_{cor} are the observed and the corrected fluorescences; and A_{ex} and A_{em} are the excitation and emission wavelengths, respectively.

The spectra were obtained for the ETB and BSA for the binary and the ternary system separately. The BSA-ETB was termed the binary system and the ternary system when it consisted of BSA-ETB and three flavonoids: RUT, NAR, and SIN.

All the spectra were obtained at a constant BSA concentration of 1.5 μM. The concentration for ETB was varied from 0.00 to 27.5 μM in both the systems. However, in the ternary system, a fixed concentration 5.5 μM of RUT, NAR, and SIN was added to the BSA and was followed by ETB interaction. The BSA-ETB system spectra were obtained at three different temperatures (298, 303, and 310 K) to explore the interaction mechanism. The binary-system interaction at 298 K was compared to the ternary system.

2.3. U.V. Absorption Measurements

The UV-Visible spectrophotometer 1800 (Shimadzu, Kyoto, Japan) was used to obtain the spectra for the BSA-ETB binary system and the ternary system. The BSA concentration was kept constant for all the experiments (1.5 μM) while the ETB concentration ranged from 0.00–10 μM for both binary and ternary systems. The RUT, NAR, and SIN concentrations were 5.5 μM in the ternary system.

2.4. Molecular Docking

The software (MOE-2015) used was a molecular operating environment (MOE, Montreal, QC, Canada) to evaluate the docking between BSA, ETB and RUT, NAR, and SIN. The BSA

crystalline structure (PDB ID: 4F5S) was retrieved from the protein data bank (rcsb.org). The ligand structures ETB (PUBCHEM ID: 176870), RUT (PUBCHEM ID: 5280805), NAR (PUBCHEM ID: 932), and SIN (PUBCHEM ID: 637775), were retrieved form the PubChem in SDF format and then converted to PDB format. The docking parameters were set as default and included the triangle matcher for the replacement procedure, and for the scoring function, London dG was used. Finalization of the scoring was performed with the GBV1/WSA dG algorithm. The ligands ETB, RUT, NAR, and SIN were allowed to dock with the BSA at the three binding regions in the subdomain IIA, IIIA, and IB for the binary system. For the docking of the ternary system, the flavonoids were first docked with BSA to obtain a right conformation of the protein and flavonoids (RUT/NAR/SIN). The BSA-flavonoid system was then docked with ETB, where BSA-RUT, BSA-NAR, and BSA-SIN acted as the protein receptors. The most suitable protein-ligand docking conformation was selected for evaluation.

3. Results and Discussion

3.1. Fluorescence Quenching and Enhancement

The binary- and the ternary-system spectra were obtained at an excitation wavelength of 280 nm, while the emission wavelength ranged between 300–500 nm (Figure 2A–D). The binary-system spectra showed a decline in the fluorescence intensity with the addition of ETB to BSA. The fluorescence intensity declined further with the increase in the ETB concentration (Figure 2A). The decline in fluorescence intensity in the ternary system, including the flavonoids RUT, NAR, and SIN, decreased further than the binary system (Figure 2B–D). The spectra for the BSA-ETB system showed a redshift of 7 nm in the emission, suggesting increased polarity and reduced hydrophobicity of the fluorophore amino acids [29,30]. The mechanism of quenching behavior of the BSA-ETB system was obtained from the Stern Volmer plot using the Stern Volmer equation [31]:

$$\frac{F_0}{F} = 1 + K_{sv}[Q] = 1 + k_q \tau_0 [Q]$$

$$k_q = K_{sv}/\tau_0$$

The fluorescence intensity of BSA is F_0, and the fluorescence intensity of the protein-ligand (BSA-ETB) is *F*. K_{sv} is the Stern Volmer constant, and [*Q*] is the quencher concentration. The biomolecular quenching constant is *kq*, and the fluorophore lifetime τ_0 for BSA in quencher absence is 6 ns.

The Stern Volmer plot of the BSA-ETB system showed declined quenching constant K_{sv} values with the elevated temperature (Table 1). The Stern Volmer plots at the three studied temperatures were linear (Figure 3A). In static or dynamic quenching, K_{sv} decreases or increases, respectively, with a temperature rise. Since the BSA-ETB system showed reduced K_{sv} values with increased temperature, the BSA-ETB system followed a static-quenching mechanism [31,32]. Further, the static quenching also suggests the formation of a stable complex between the two of them. The biomolecular quenching constant values provide a tool to establish the quenching mechanism. The static-quenching behavior of the BSA-ETB complex for the binary system is predicted based on the biomolecular quenching constant values that were higher than 2×10^{10} L mol^{-1} s^{-1} (Table 1). It is already well-known that k_q values more than the 2×10^{10} L mol^{-1} s^{-1} suggest a static quenching, whereas the values below indicate a dynamic quenching between binary systems [31,32].

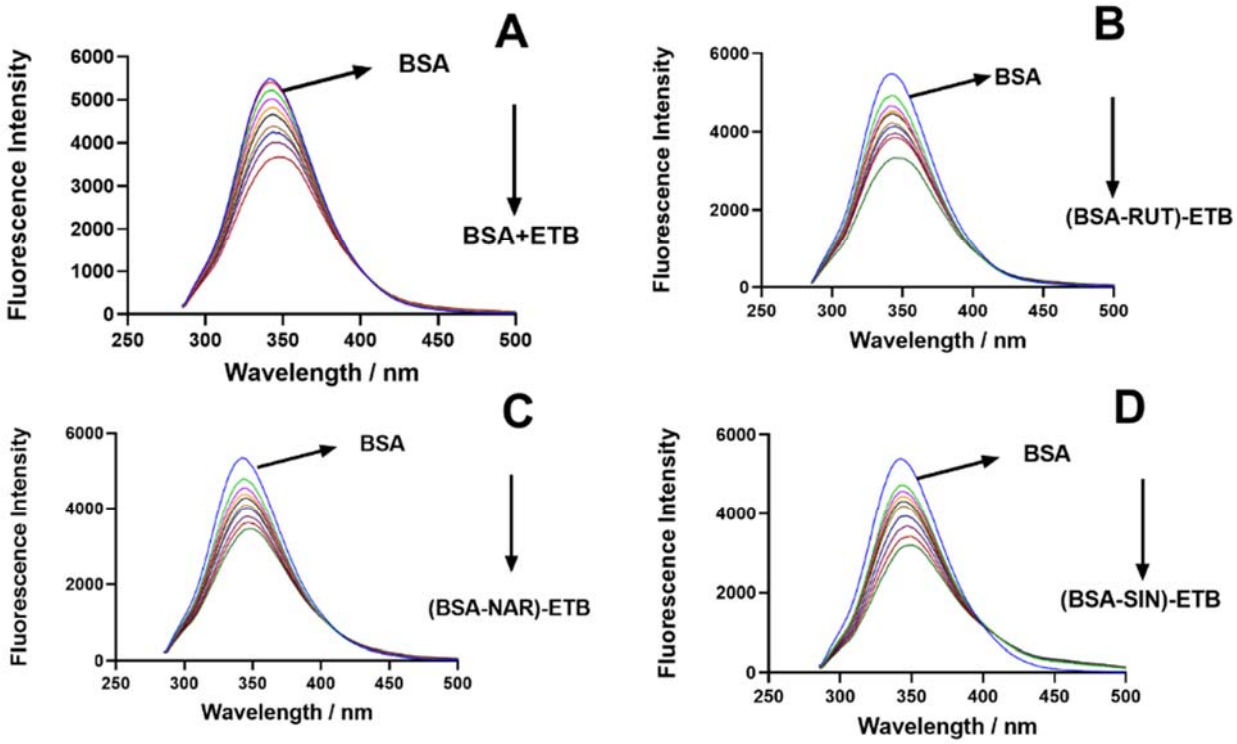

Figure 2. The fluorescence spectra of the (**A**): BSA-ETB binary system and BSA-ETB ternary system in presence of flavonoids, (**B**): RUT; (**C**): NAR; and (**D**): SIN). BSA (1.5 μM) with a: ETB (0.00–27.5 μM); and (RUT, NAR, and SIN) = 5.5 μM at (λ_{ex} = 280 nm and λ_{em} = 300–500 nm).

Table 1. Stern Volmer K_{sv} and bimolecular quenching constant k_q.

T (K)	R	$K_{sv} \times 10^4 \pm$ SD (M^{-1})	$k_q \times 10^{12}$ (M^{-1} S^{-1})
298	0.9890	1.88	3.14
303	0.9888	1.78	2.97
307	0.9966	1.74	2.90

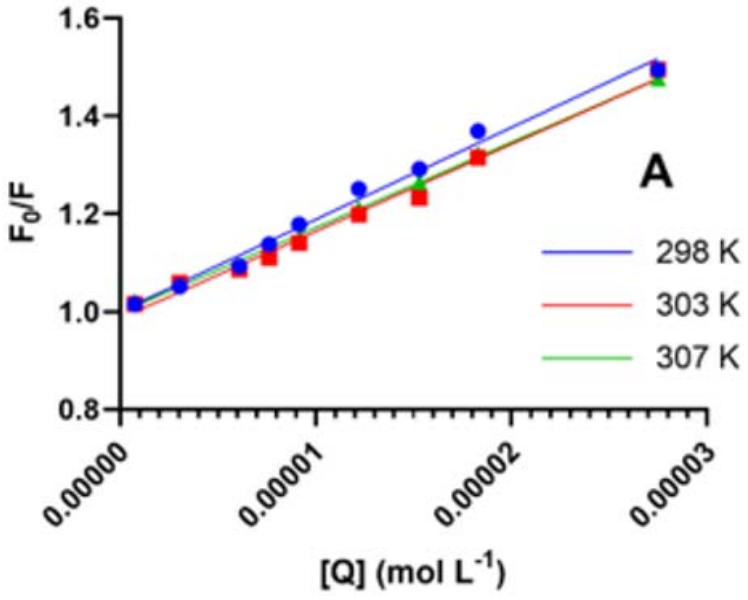

Figure 3. *Cont.*

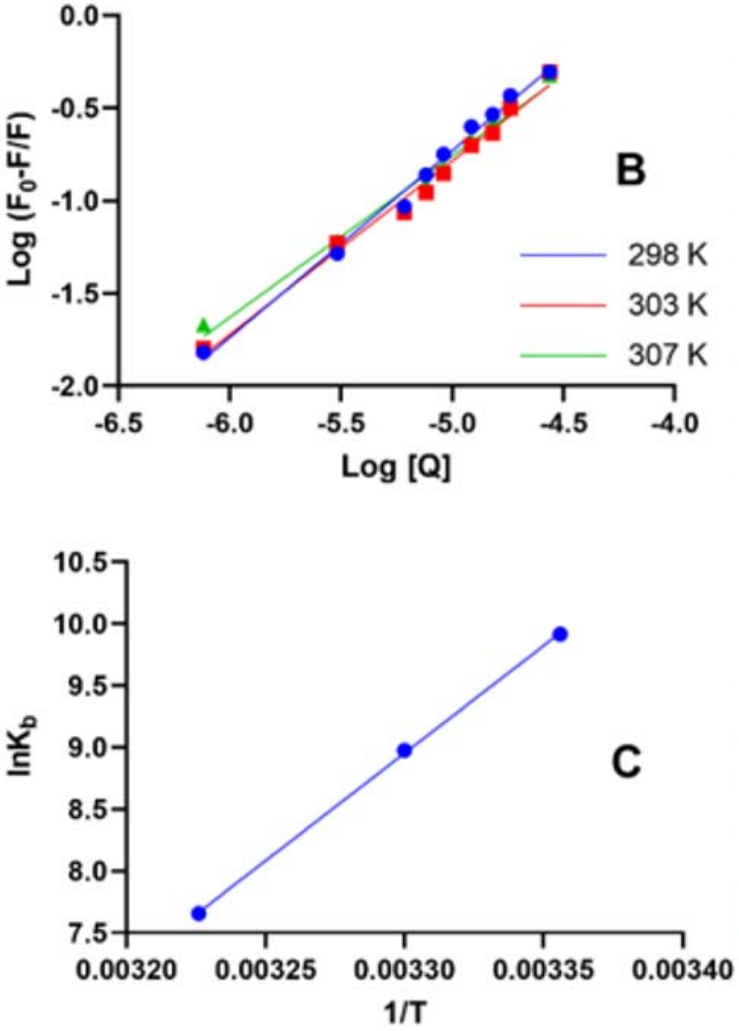

Figure 3. (**A**): Stern Volmer Plot (**B**): binding constant from double reciprocal plot (**C**): van't Hoff plots for thermodynamic parameters for BSA (1.5 µM)-ETB (0.00–27.5 µM) system at 298/303/310 K.

The K_{sv} and k_q were also evaluated for the ternary system for the BSA-ETB in the presence of RUT, NAR, and SIN (Table 2). The effect of the ternary system was determined by the Stern Volmer constant and biomolecular quenching constant values. These values were later compared to the binary BSA-ETB system.

Table 2. Quenching constants of the binary and ternary systems at room temperature.

System	k_q (M^{-1} S^{-1})	K_b
BSA-ETB	3.14×10^{12}	2.02×10^{4}
(BSA-RUT)-ETB	4.60×10^{12}	1.12×10^{2}
(BSA-NAR)-ETB	6.21×10^{12}	1.61×10^{3}
(BSA-SIN)-ETB	4.35×10^{12}	1.02×10^{3}

3.2. Binding Constant and Number of Binding Sites

The Hill equation was applied to calculate the binding constant and cooperativity of ligand binding to BSA for both the binary and ternary systems.

$$\log \frac{(F_0 - F)}{F} = \log K_b + n \ \log[\mathrm{Q}]$$

Here in this equation, K_b represents the binding constant, and n is the cooperativity factor. There is no cooperativity when n equals 1; thus, $n < 1$ shows negative cooperativity, $n = 1$, $n > 1$ shows positive cooperativity. The binding constants of the BSA-ETB system at the respective temperatures are shown in Table 3 and Figure 3B. The binding constants for the BSA-ETB decreased with the temperature rise. The binding cooperativity $n = 1$ was found for the BSA-ETB system at 273 K, which suggests no influence on the binding cooperativity for the binary system at 298 K. Further, it was also observed for the BSA-ETB system that as the temperature increased, the binding cooperativity decreased ($n < 1$) and, therefore, negative cooperativity. A medium binding affinity between ETB and BSA is suggested based on the obtained values of 10^4 M^{-1} [33]. The binding constant values of the ternary system, BSA-ETB, in the presence of the three flavonoids RUT, NAR, and SIN, showed a decline in the values compared to the binary system. The BSA-ETB interaction was further studied at different temperatures to determine the thermodynamics of the reactions by the following:

$$\ln K_b = -\frac{\Delta H^\circ}{RT} + \frac{\Delta S^\circ}{R}$$

$$\Delta G^\circ = \Delta H^\circ - T\Delta S^\circ$$

where ΔH° is enthalpy change, ΔS° is entropy change, ΔG° is Gibbs free energy, R is the universal gas constant, and T is the temperature in kelvins (K). A van't Hoff plot between $\ln(K_b)$ vs. $1/T$ (Figure 3C) predicted ΔH°, ΔS°, and ΔG° values (Table 3). The negative ΔG° suggested a spontaneous complex formation between ETB and BSA. Furthermore, the negative values of enthalpy, as well as entropy, indicated van der Waals interaction and hydrogen bonds playing a role in complex formation between BSA and ETB.

Table 3. Binding parameters and thermodynamic parameters for BSA-ETB system.

T (K)	$K_b \pm$ SD	n	$\Delta G^\circ \pm$ SD (kJ mol^{-1})	$\Delta H^\circ \pm$ SD (kJ mol^{-1})	$\Delta S^\circ \pm$ SD (J mol^{-1}·K^{-1})
298	2.02×10^4	1.0073	−24.59		
303	7.91×10^3	0.9871	−22.57	−144.69	−403.02
307	2.12×10^3	0.9833	−20.96		

3.3. Comparison of Binary and Ternary-System Interactions

The binding constants were compared to each other for both the ternary and binary systems. A decrease in the binding constants was observed with a temperature rise in the binary system compared to the ternary system. It was observed that the addition of the flavonoids in the BSA-ETB system interfered in the binding and quenching constants of the BSA-ETB system (Table 2). The interaction with flavonoids (RUT, NAR, and SIN) and BSA was previously reported to decrease albumin fluorescence, and the binding constants for the three flavonoids RUT, NAR, and SIN were of the magnitude of >106, >104, and >105, respectively [34–37]. The presence of RUT, NAR, and SIN increased the quenching constants in the ternary system. In the binary system, ETB quenched the fluorescence of the serum albumin by 27%, while as in the ternary system, RUT, NAR, and SIN in the ETB quenched the fluorescence of serum albumin by 29%, 33%, and 37%, respectively (Figure 4). Therefore, the influence of the studied flavonoids varied, with RUT affecting the least followed by NAR and the highest with SIN. The elevated quenching constants for the ternary system suggest that RUT, NAR, and SIN might have increased the accessibility of the ETB to the BSA, improving its quenching efficiency or the flavonoids had a synergistic effect. Hence, the quenching increased (Table 2) [38].

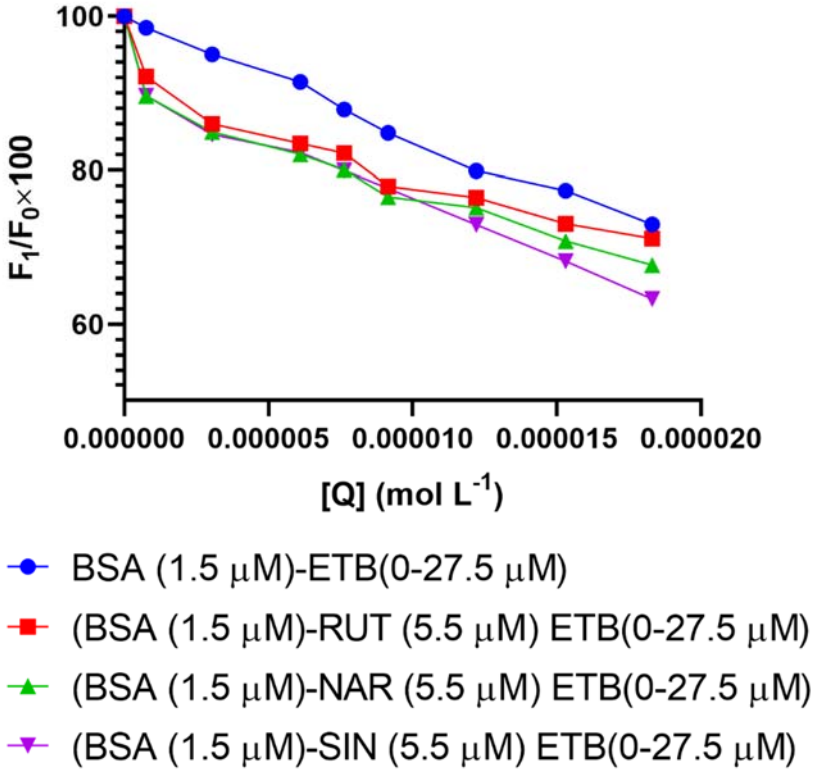

Figure 4. Quenching curves BSA and ETB in presence and absence of flavonoids.

The results from the present study corroborate earlier studies where a moderate binding between BSA and ETB was established [32], and the temperature rise led to a further decrease in the binding constants. In addition, interaction studies of BSA with the RUT, NAR, and SIN have established that RUT and SIN bind very firmly to BSA with binding constants greater than 10^5 $M^{-1,}$ whereas NAR is moderately bound to BSA [34–37]. Hence, the binding constants for the BSA-ETB system were calculated for the ternary system separately for RUT, NAR, and SIN since the studied flavonoids either strongly or moderately interact with BSA, which may, in turn, influence the ETB binding to BSA as it is moderately bound to BSA. As is apparent from (Table 2), the binding constant values of the ternary system were less than that of the binary system. Further, the binding cooperativity obtained from the Hill equation is less than one, which suggests negative cooperativity. Hence, the presence of RUT, NAR, and SIN in the BSA-ETB system lowers the affinity of the ETB towards BSA. In addition, it suggests that ternary-complex formation is less favorable than the ligands binding independently. Thus, the effect of RUT, NAR, and SIN in the systemic circulation might increase the free ETB fraction.

The high plasma-ETB concentration has been associated with some severe adverse events in patients on ETB therapeutic regimens. Furthermore, adherence to the ETB treatment regimen has been affected by the severe adverse effects in NSCLC patients, which may be related to therapeutic plasma-ETB concentrations [39]. Some of the common adverse events associated with ETB use are skin-related, including acne, rash, pruritus, xeroderma, and paronychia. These adverse events sometimes become severe, which necessitate disruption or complete termination of the treatment with ETB [40]. High plasma-ETB concentration is one of the reasons leading to the severe adverse events associated with ETB and affects patients' adherence to the therapeutic regimen. In addition, the presence of RUT, NAR, and SIN impacts the binding constant of ETB, which infers that they may affect the plasma concentrations of ETB, leading to severe adverse events and cessation of treatment.

3.4. UV-Absorption Studies

The protein-ligand interaction gives information about the structural changes in the complex formed during the interaction and the protein alone. Static quenching leads to changes in the structure, and hence, the protein spectra on interaction with its ligand. Based on our results, the static quenching was predicted between BSA and ETB. The λmax of BSA was at 280 nm because of $\pi - \pi^*$ transitions in the aromatic amino acids (tryptophan, tyrosine, and phenylalanine). On the interaction of the BSA with ETB, the λmax shifted to 330 nm (Figure 5A) [31,41]. The hyperchromicity at 280 nm also suggested complex formation between ETB and BSA.

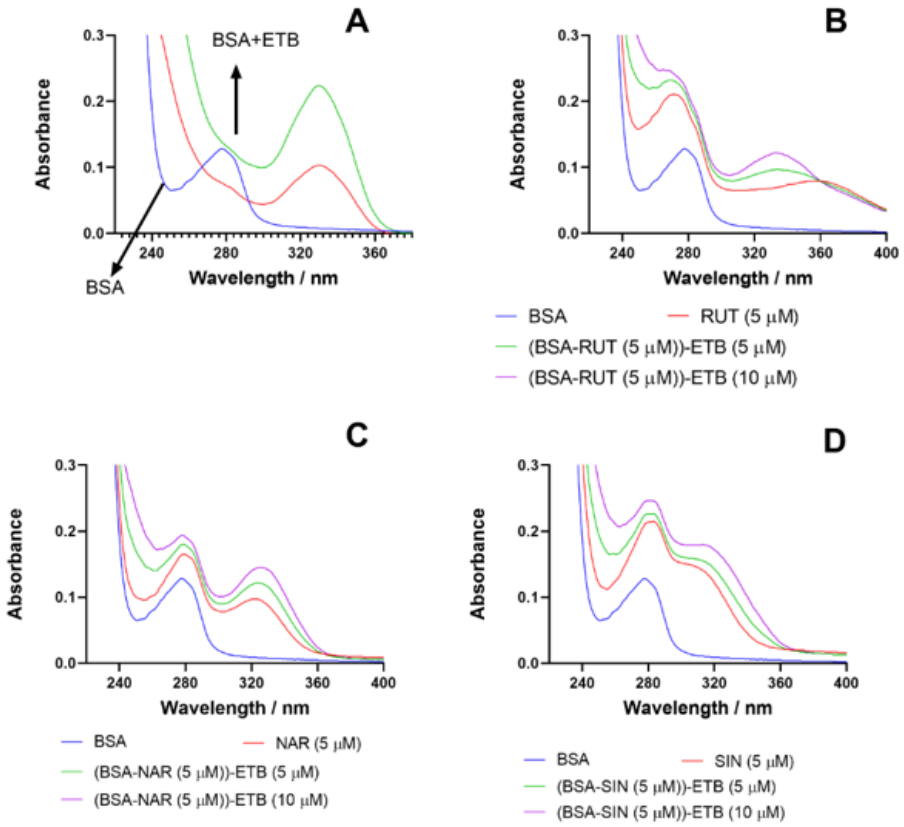

Figure 5. Ultraviolet-visible spectra for (**A**): BSA (1.5 μM) in presence and absence of ETB (0.00–10 μM) and in presence of (**B**): RUT; (**C**): NAR; (**D**): SIN.

The BSA-ETB spectra were also recorded for each RUT, NAR, and SIN to observe if any difference in the spectra of BSA occurs in the presence of these flavonoids (Figure 5B–D). The BSA showed hyperchromicity on interaction with ETB in the presence of RUT, NAR, and SIN. The spectra for the ternary system of BSA-ETB were significantly different from those of the BSA-ETB spectra binary system. Hence, the binary and the ternary-system complexes formed were completely different from one another. Further comparing the ternary systems amongst themselves, the spectra differed from each other and thus inferred that complexes formed between BSA-ETB in the presence of RUT, NAR, and SIN were also different.

3.5. Molecular Docking

The experimental results were supplemented with molecular-docking analysis using MOE. Experimental results suggested that the binding site for ETB binding on BSA to be Site I (subdomain IIA) and Site III (subdomain IIB) [26,42] (Figure 6A,B). Blind docking in silico was performed for the BSA-ETB system, and the results of the binary system were compared to the ternary-system docking for the BSA-ETB in the presence of RUT, NAR,

and SIN. It was observed that ETB binds to subdomain IIA and subdomain IB of BSA in corroboration with previous studies. The molecular docking results are presented in Table 4 and suggest high binding energy for the BSA-ETB system at subdomain IIA. The binding energy showed a decline in the presence of all the flavonoids RUT, NAR, and SIN, with the highest value of reduction in the binding energy in RUT, followed by SIN and then NAR. Thus, the presence of the three drugs RUT, NAR, and SIN influenced the binding energy of ETB with BSA.

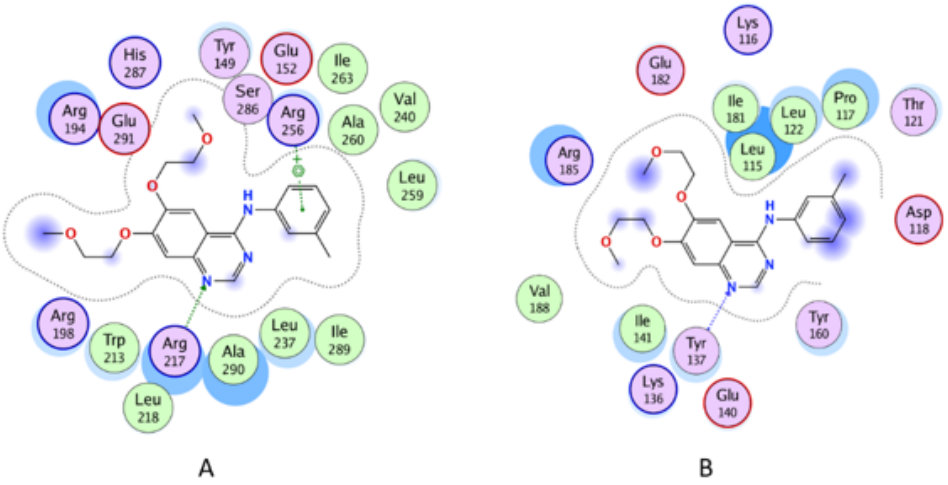

Figure 6. Two-dimensional molecular-docking conformation for BSA ETB system (**A**): Site I and (**B**): Site III.

Table 4. Molecular-docking results for the binary and ternary BSA-ETB systems.

Complex	Ligand	Receptor				Interaction	Distance	Score Kcal mol^{-1}	Subdomain
ETB-BSA	*n*33	CD	ARG	217	(A)	H-acceptor	3.39	−9.255	IIA
	6-ring	NE	ARG	256	(A)	pi-cation	3.8		
ETB(BSA-NRN)	O14	OG	SER	286	(A)	H-donor	3.14	−7.684	
	O1	NE	ARG	217	(A)	H-acceptor	3.04		
ETB(BSA-RTN)	N38	OD2	ASP	450	(A)	H-donor	3.18	−6.331	
	N33	CE	LYS	439	(A)	H-acceptor	3.51		
ETB(BSA-SPA)	C29	5-ring	HIS	287	(A)	H-pi	4.15	−7.428	
	6-ring	CD	ARG	194	(A)	pi-H	3.15		
	6-ring	NH1	ARG	198	(A)	pi-cation	4.31		
ETB-BSA	N33	CA	TYR	137	(A)	H-acceptor	3.49	−7.495	IB
ETB(BSA-NRN)	O28	NE	ARG	427	(A)	H-acceptor	3.21	−6.836	
	6-ring	CD	PRO	110	(A)	pi-H	4.53		
ETB(BSA-RTN)	O5	NZ	LYS	114	(A)	H-acceptor	2.87	−7.272	
	O28	NH1	ARG	185	(A)	H-acceptor	3.13		
	O28	NH2	ARG	185	(A)	H-acceptor	2.97		
ETB(BSA-SPA)	O5	NH2	ARG	185	(A)	H-acceptor	2.93	−7.056	
	6-ring	N	LEU	115	(A)	pi-H	4.41		
	6-ring	CB	ARG	144	(A)	pi-H	4.22		
	6-ring	CD	ARG	144	(A)	pi-H	4.04		

Further, the comparison was made in the binding energies at subdomain IB, and it was observed that the binding energies for the BSA-ETB system in the presence of RUT, NAR, and SIN were lower than the BSA-ETB system in their absence, as shown in Table 4.

The amino acids Glu291, Leu218, Glu152, Arg198, Arg256, Arg217, Ser286, Leu237, Leu259, Ile289, Tyr149, Ile263, Ala290, Trp213, Ala260, Val240, and Arg194 in the vicinity of the ETB at the binding site in subdomain IIA surrounded the binding pocket at subdomain IB with amino acids Lys 116, Pro117, Leu115, Ile181, Leu122, Glu182, Tyr137, Lys136, Arg185, Ile141, Tyr160, Val188, Glu140, Asp118, and Thr121. A hydrogen bond and pi-cation bonds were involved in the formation of the binary complex between BSA and ETB at Site I, whereas one hydrogen bond was involved in the interaction between BSA and ETB at site III. The changes in the bonding in the ternary complex due to RUT, NAR, and SIN are given in Table 4 and Figure 7A–C. The three-dimensional figures for the interaction studies have been given in the Supplementary Materials (Figure S1). Molecular dynamic simulation studies conducted for the BSA-STB system suggested no fluctuation in the RMSD and RMSF plots of BSA-ETB and concluded a stable complex formation between BSA and ETB [26].

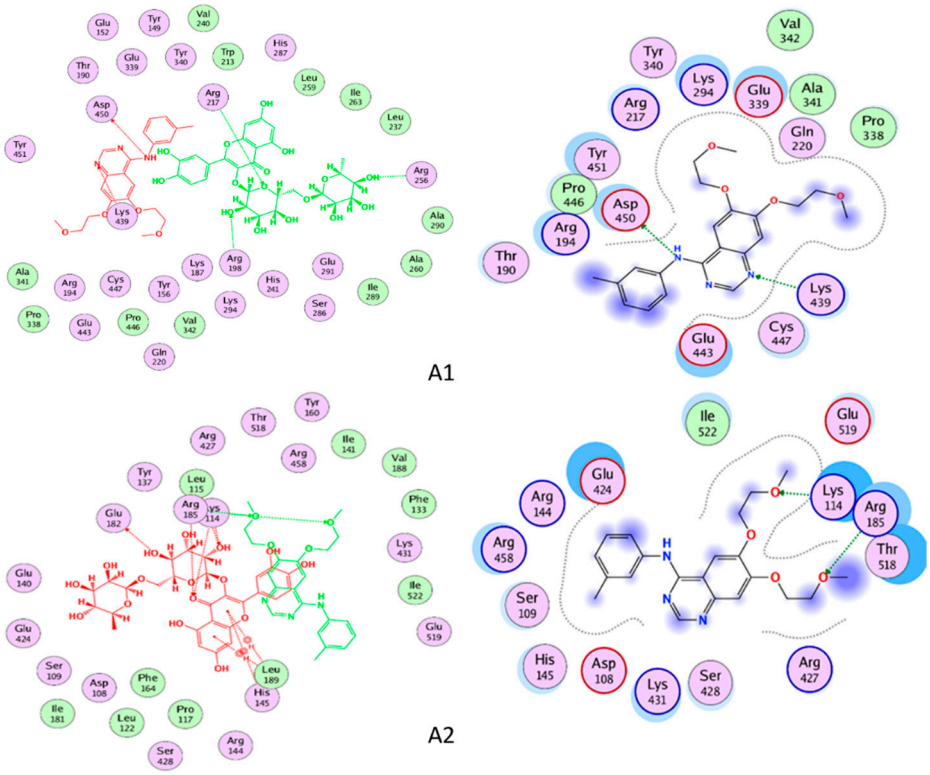

Figure 7. *Cont.*

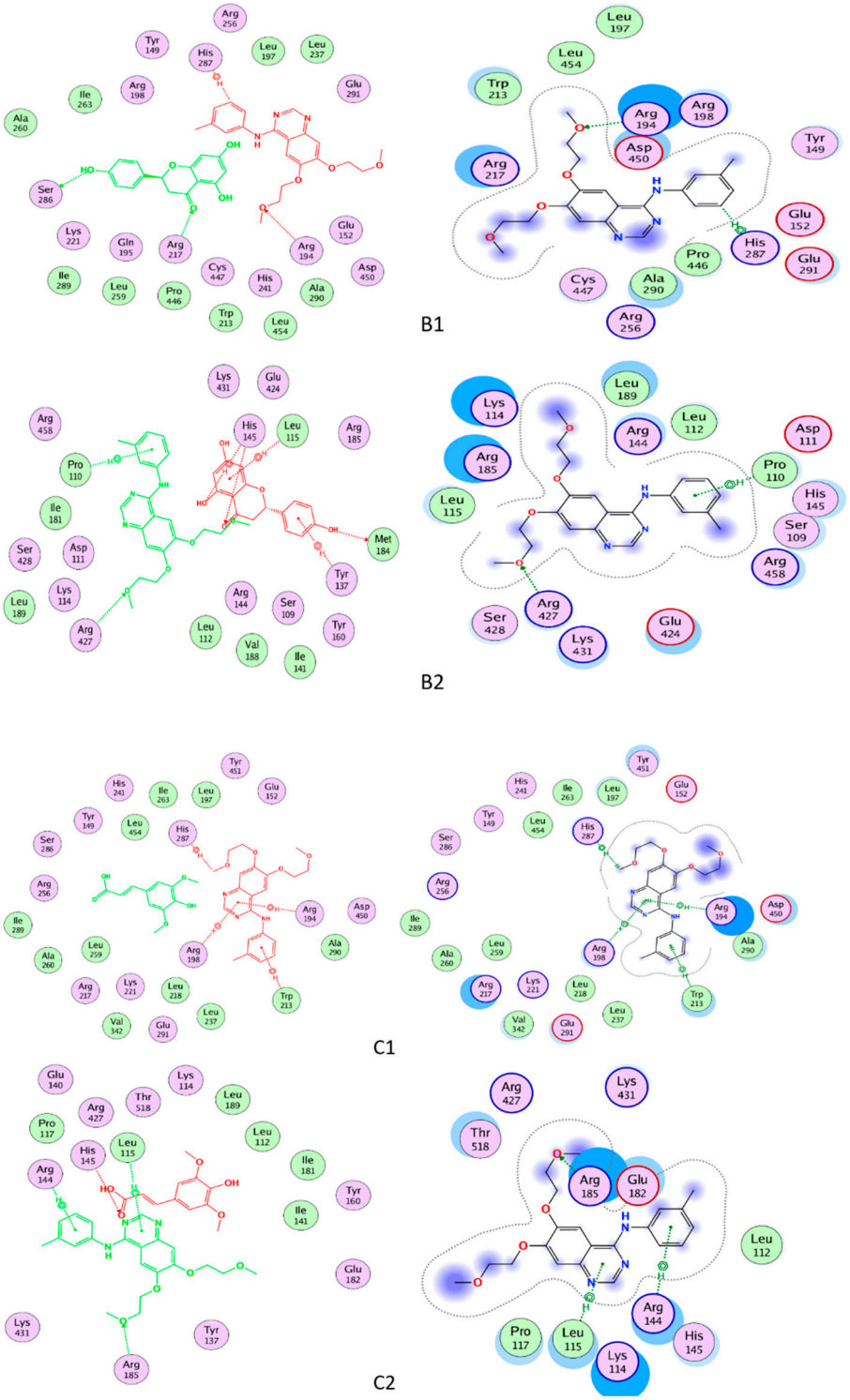

Figure 7. Two-dimensional molecular-docking conformation for BSA ETB. In presence of RUT, (**A1**): Site I, (**A2**): Site III, In presence of NAR, (**B1**): Site I, (**B2**): Site III; In presence of SIN, (**C1**): Site I, (**C2**): Site III.

4. Conclusions

The present research studied the influence of three flavonoids—RUT, NAR, and SIN—on the binding complex formed between ETB with BSA. The study design consisted of both experimental as well as computational approaches to predict the molecular mechanism involved in the interactions. A reduction in the binding constant of the BSA-ETB binary system was evaluated in the presence of all the three ligands—RUT, NAR, and SIN—in

the ternary system. The free drug fraction of ETB might be altered in the presence of RUT, NAR, and SIN. Furthermore, the nonadherence to the treatment regimen of ETB is associated with some severe dermatological side effects, which are further associated with the systemic concentration of ETB. Hence, coadministration of these flavonoids might influence the pharmacokinetic behavior of ETB, and their further knowledge needs to be explored in vivo.

Supplementary Materials: The following supporting information can be downloaded at: https://www.mdpi.com/article/10.3390/app12073575/s1, Figure S1: Three dimensional conformations for BSA-ETB in absence and in presence of RUT, NAR and SIN at Site I and Site III of BSA.

Author Contributions: Conceptualization: T.A.W., S.Z.; Methodology: T.A.W., S.Z.; Software: A.H.B.; Formal analysis: A.I.A.K., S.Z.; Investigation: A.H.B., T.A.W., S.Z., A.A.A.-M.; Resources: T.A.W.; Writing: S.Z., T.A.W.; Review & Editing: A.I.A.K., A.A.A.-M., T.A.W. Project administration: T.A.W. All authors have read and agreed to the published version of the manuscript.

Funding: Researchers Supporting Project number (RSP-2021/357), King Saud University, Riyadh, Saudi Arabia.

Institutional Review Board Statement: Not Applicable.

Informed Consent Statement: Not Applicable.

Data Availability Statement: Data will be available on request to corresponding author.

Acknowledgments: The authors extend their appreciation to Researchers Supporting Project number (RSP-2021/357), King Saud University, Riyadh, Saudi Arabia, for funding this work.

Conflicts of Interest: The authors declare no conflict of interest.

References

1. Peters, T., Jr. *All about Albumin: Biochemistry, Genetics, and Medical Applications*; Academic Press: Cambridge, MA, USA, 1995.
2. Wang, B.-L.; Kou, S.-B.; Lin, Z.-Y.; Shi, J.-H. Investigation on the binding behavior between BSA and lenvatinib with the help of various spectroscopic and in silico methods. *J. Mol. Struct.* **2020**, *1204*, 127521. [CrossRef]
3. Koch-Weser, J.; Sellers, E.M. Binding of drugs to serum albumin. *N. Engl. J. Med.* **1976**, *294*, 311–316. [CrossRef] [PubMed]
4. Keller, F.; Maiga, M.; Neumayer, H.-H.; Lode, H.; Distler, A. Pharmacokinetic effects of altered plasma protein binding of drugs in renal disease. *Eur. J. Drug Metab. Pharmacokinet.* **1984**, *9*, 275–282. [CrossRef] [PubMed]
5. Ni, Y.; Su, S.; Kokot, S. Spectrofluorimetric studies on the binding of salicylic acid to bovine serum albumin using warfarin and ibuprofen as site markers with the aid of parallel factor analysis. *Anal. Chim. Acta* **2006**, *580*, 206–215. [CrossRef]
6. Wani, T.A.; Alsaif, N.; Bakheit, A.H.; Zargar, S.; Al-Mehizia, A.A.; Khan, A.A. Interaction of an abiraterone with calf thymus DNA: Investigation with spectroscopic technique and modelling studies. *Bioorgan. Chem.* **2020**, *100*, 103957. [CrossRef]
7. Fan, J.; Sun, W.; Wang, Z.; Peng, X.; Li, Y.; Cao, J. A fluorescent probe for site I binding and sensitive discrimination of HSA from BSA. *Chem. Commun.* **2014**, *50*, 9573–9576. [CrossRef]
8. Zhang, Y.-F.; Zhou, K.-L.; Lou, Y.-Y.; Pan, D.-q.; Shi, J.-H. Investigation of the binding interaction between estazolam and bovine serum albumin: Multi-spectroscopic methods and molecular docking technique. *J. Biomol. Struct. Dyn.* **2017**, *35*, 3605–3614. [CrossRef]
9. Fanali, G.; Di Masi, A.; Trezza, V.; Marino, M.; Fasano, M.; Ascenzi, P. Human serum albumin: From bench to bedside. *Mol. Asp. Med.* **2012**, *33*, 209–290. [CrossRef]
10. Sudlow, G.; Birkett, D.J.; Wade, D.N. Spectroscopic techniques in the study of protein binding. A fluorescence technique for the evaluation of the albumin binding and displacement of warfarin and warfarin-alcohol. *Clin. Exp. Pharmacol. Physiol.* **1975**, *2*, 129–140. [CrossRef]
11. He, X.M.; Carter, D.C. Atomic structure and chemistry of human serum albumin. *Nature* **1992**, *358*, 209–215. [CrossRef]
12. Wani, T.A.; Alsaif, N.; Alanazi, M.M.; Bakheit, A.H.; Zargar, S.; Bhat, M.A. A potential anticancer dihydropyrimidine derivative and its protein binding mechanism by multispectroscopic, molecular docking and molecular dynamic simulation along with its in-silico toxicity and metabolic profile. *Eur. J. Pharm. Sci.* **2021**, *158*, 105686. [CrossRef]
13. Wani, T.A. Highly sensitive ultra-performance liquid chromatography–tandem mass spectrometry method for the determination of abiraterone in human plasma. *Anal. Methods* **2013**, *5*, 3693–3699. [CrossRef]
14. Khalil, N.Y.; Wani, T.A.; Abunassif, M.A.; Darwish, I.A. Sensitive HPLC method with fluorescence detection and on-line wavelength switching for simultaneous determination of valsartan and amlodipine in human plasma. *J. Liq. Chromatogr. Rel. Technol.* **2011**, *34*, 2583–2595. [CrossRef]

15. Jing, J.J.; Liu, B.; Wang, X.; Wang, X.; He, L.L.; Guo, X.Y.; Xu, M.L.; Li, Q.Y.; Gao, B.; Dong, B.Y. Binding of fluphenazine with human serum albumin in the presence of rutin and quercetin: An evaluation of food-drug interaction by spectroscopic techniques. *Luminescence* **2017**, *32*, 1056–1065. [CrossRef]
16. Alsaif, N.A.; Al-Mehizia, A.A.; Bakheit, A.H.; Zargar, S.; Wani, T.A. A spectroscopic, thermodynamic and molecular docking study of the binding mechanism of dapoxetine with calf thymus DNA. *S. Afr. J. Chem.* **2020**, *73*, 44–50. [CrossRef]
17. Benet, L.Z.; Bowman, C.M.; Sodhi, J.K. How transporters have changed basic pharmacokinetic understanding. *AAPS J.* **2019**, *21*, 103. [CrossRef]
18. Zargar, S.; Wani, T.A. Protective Role of Quercetin in Carbon Tetrachloride Induced Toxicity in Rat Brain: Biochemical, Spectrophotometric Assays and Computational Approach. *Molecules* **2021**, *26*, 7526. [CrossRef]
19. Frutos, M.J.; Rincón-Frutos, L.; Valero-Cases, E. Rutin. In *Nonvitamin and Nonmineral Nutritional Supplements*; Elsevier: Amsterdam, The Netherlands, 2019; pp. 111–117.
20. Farha, A.K.; Gan, R.-Y.; Li, H.-B.; Wu, D.-T.; Atanasov, A.G.; Gul, K.; Zhang, J.-R.; Yang, Q.-Q.; Corke, H. The anticancer potential of the dietary polyphenol rutin: Current status, challenges, and perspectives. *Crit. Rev. Food Sci. Nutr.* **2022**, *62*, 832–859. [CrossRef]
21. Cavia-Saiz, M.; Busto, M.D.; Pilar-Izquierdo, M.C.; Ortega, N.; Perez-Mateos, M.; Muñiz, P. Antioxidant properties, radical scavenging activity and biomolecule protection capacity of flavonoid naringenin and its glycoside naringin: A comparative study. *J. Sci. Food Agric.* **2010**, *90*, 1238–1244. [CrossRef]
22. Kumar, S.P.; Birundha, K.; Kaveri, K.; Devi, K.R. Antioxidant studies of chitosan nanoparticles containing naringenin and their cytotoxicity effects in lung cancer cells. *Int. J. Biol. Macromol.* **2015**, *78*, 87–95. [CrossRef]
23. Pandi, A.; Kalappan, V.M. Pharmacological and therapeutic applications of Sinapic acid—An updated review. *Mol. Biol. Rep.* **2021**, *48*, 3733–3745. [CrossRef] [PubMed]
24. Park, J.H.; Liu, Y.; Lemmon, M.A.; Radhakrishnan, R. Erlotinib binds both inactive and active conformations of the EGFR tyrosine kinase domain. *Biochem. J.* **2012**, *448*, 417. [CrossRef] [PubMed]
25. Zhou, X.; Shi, K.; Hao, Y.; Yang, C.; Zha, R.; Yi, C.; Qian, Z. Advances in nanotechnology-based delivery systems for EGFR tyrosine kinases inhibitors in cancer therapy. *Asian J. Pharm. Sci.* **2020**, *15*, 26–41. [CrossRef] [PubMed]
26. Wani, T.A.; Alanazi, M.M.; Alsaif, N.A.; Bakheit, A.H.; Zargar, S.; Alsalami, O.M.; Khan, A.A. Interaction Characterization of a Tyrosine Kinase Inhibitor Erlotinib with a Model Transport Protein in the Presence of Quercetin: A Drug–Protein and Drug–Drug Interaction Investigation Using Multi-Spectroscopic and Computational Approaches. *Molecules* **2022**, *27*, 1265. [CrossRef]
27. Wani, T.A.; Bakheit, A.H.; Al-Majed, A.A.; Altwaijry, N.; Baquaysh, A.; Aljuraisy, A.; Zargar, S. Binding and drug displacement study of colchicine and bovine serum albumin in presence of azithromycin using multispectroscopic techniques and molecular dynamic simulation. *J. Mol. Liq.* **2021**, *333*, 115934. [CrossRef]
28. Sengupta, B.; Sengupta, P.K. The interaction of quercetin with human serum albumin: A fluorescence spectroscopic study. *Biochem. Biophys. Res. Commun.* **2002**, *299*, 400–403. [CrossRef]
29. Xie, L.; Wehling, R.L.; Ciftci, O.; Zhang, Y. Formation of complexes between tannic acid with bovine serum albumin, egg ovalbumin and bovine beta-lactoglobulin. *Food Res. Int.* **2017**, *102*, 195–202. [CrossRef]
30. Al-Mehizia, A.A.; Bakheit, A.H.; Zargar, S.; Bhat, M.A.; Asmari, M.M.; Wani, T.A. Evaluation of biophysical interaction between newly synthesized pyrazoline pyridazine derivative and bovine serum albumin by spectroscopic and molecular docking studies. *J. Spectrosc.* **2019**, *2019*, 3848670. [CrossRef]
31. Lakowicz, J.R. *Principles of Fluorescence Spectroscopy*; Springer Science & Business Media: Cham, Switzerland, 2013.
32. Rasoulzadeh, F.; Asgari, D.; Naseri, A.; Rashidi, M.R. Spectroscopic studies on the interaction between erlotinib hydrochloride and bovine serum albumin. *DARU J. Pharm. Sci.* **2010**, *18*, 179.
33. Wani, T.A.; Bakheit, A.H.; Zargar, S.; Bhat, M.A.; Al-Majed, A.A. Molecular docking and experimental investigation of new indole derivative cyclooxygenase inhibitor to probe its binding mechanism with bovine serum albumin. *Bioorgan. Chem.* **2019**, *89*, 103010. [CrossRef]
34. Zargar, S.; Alamery, S.; Bakheit, A.H.; Wani, T.A. Poziotinib and bovine serum albumin binding characterization and influence of quercetin, rutin, naringenin and sinapic acid on their binding interaction. *Spectrochim. Acta Part A Mol. Biomol. Spectrosc.* **2020**, *235*, 118335. [CrossRef]
35. Sengupta, P.; Sardar, P.S.; Roy, P.; Dasgupta, S.; Bose, A. Investigation on the interaction of Rutin with serum albumins: Insights from spectroscopic and molecular docking techniques. *J. Photochem. Photobiol. B Biol.* **2018**, *183*, 101–110. [CrossRef]
36. Hu, Y.-J.; Wang, Y.; Ou-Yang, Y.; Zhou, J.; Liu, Y. Characterize the interaction between naringenin and bovine serum albumin using spectroscopic approach. *J. Lumin.* **2010**, *130*, 1394–1399. [CrossRef]
37. Sengupta, P.; Pal, U.; Mondal, P.; Bose, A. Multi-spectroscopic and computational evaluation on the binding of sinapic acid and its Cu (II) complex with bovine serum albumin. *Food Chem.* **2019**, *301*, 125254. [CrossRef]
38. Kameníková, M.; Furtmüller, P.G.; Klacsová, M.; Lopez-Guzman, A.; Toca-Herrera, J.L.; Vitkovská, A.; Devínsky, F.; Mučaji, P.; Nagy, M. Influence of quercetin on the interaction of gliclazide with human serum albumin–spectroscopic and docking approaches. *Luminescence* **2017**, *32*, 1203–1211. [CrossRef]
39. Timmers, L.; Boons, C.C.; Moes-Ten Hove, J.; Smit, E.F.; van de Ven, P.M.; Aerts, J.G.; Swart, E.L.; Boven, E.; Hugtenburg, J.G. Adherence, exposure and patients' experiences with the use of erlotinib in non-small cell lung cancer. *J. Cancer Res. Clin. Oncol.* **2015**, *141*, 1481–1491. [CrossRef]

40. Kiyohara, Y.; Yamazaki, N.; Kishi, A. Erlotinib-related skin toxicities: Treatment strategies in patients with metastatic non-small cell lung cancer. *J. Am. Acad. Dermatol.* **2013**, *69*, 463–472. [CrossRef]
41. Rabbani, G.; Khan, M.J.; Ahmad, A.; Maskat, M.Y.; Khan, R.H. Effect of copper oxide nanoparticles on the conformation and activity of β-galactosidase. *Colloids Surf. B. Biointerfaces* **2014**, *123*, 96–105. [CrossRef]
42. Taghipour, P.; Zakariazadeh, M.; Sharifi, M.; Dolatabadi, J.E.N.; Barzegar, A. Bovine serum albumin binding study to erlotinib using surface plasmon resonance and molecular docking methods. *J. Photochem. Photobiol. B Biol.* **2018**, *183*, 11–15. [CrossRef]